

# In Vivo Imaging in Pharmaceutical Development and Its Impact on the 3Rs

Barry R. Campbell, Dinko Gonzalez Trotter, Catherine D.G. Hines, Wenping Li, Manishkumar Patel, Weisheng Zhang, and Jeffrey L. Evelhoch

Barry R. Campbell is an Associate Principal Scientist in Translational Biomarkers at Merck Research Laboratories in Kenilworth, New Jersey. Dinko Gonzalez Trotter, PhD, is a Senior Director in Early Clinical Development at Regeneron Pharmaceuticals, Inc., in Tarrytown, New York. Catherine D. Hines, PhD is a Director in Translational Biomarkers at Merck Research Laboratories in West Point, Pennsylvania. Manishkumar Patel, PhD is a Principal Scientist in Translational Biomarkers at Merck Research Laboratories in West Point, Pennsylvania. Weisheng Zhang is a Senior Principal Scientist in Translational Biomarkers at Merck Research Laboratories in Boston, Massachusetts. Jeffrey L. Evelhoch, PhD, is Vice President of Translational Biomarkers at Merck Research Laboratories in West Point, Pennsylvania.

Address correspondence and reprint requests to Jeffrey L. Evelhoch, Merck Research Laboratories, 770 Sumneytown Pike, Mailstop: WP42-211, West Point, PA 19486 or email: jeffrey\_evelhoch@merck.com.

## Abstract

It is well understood that the biopharmaceutical industry must improve efficiency along the path from laboratory concept to commercial product. In vivo imaging is recognized as a useful method to provide biomarkers for target engagement, treatment response, safety, and mechanism of action. Imaging biomarkers have the potential to inform the selection of drugs that are more likely to be safe and effective. Most of the imaging modalities for biopharmaceutical research are translatable to the clinic. In vivo imaging does not require removal of tissue to provide biomarkers, thus reducing the number of valuable preclinical subjects required for a study. Longitudinal imaging allows for quantitative intra-subject comparisons, enhancing statistical power, and further reducing the number of subjects needed for the evaluation of treatment effects in animal models. The noninvasive nature of in vivo imaging also provides a valuable approach to alleviate or minimize potential pain, suffering or distress.

**Key words:** drug development; imaging; target engagement; treatment response; drug safety; mechanism of action; 3Rs

## Introduction

Healthcare costs have increased at an alarming rate over the past 5 decades. Spending for healthcare in the United States relative to the gross domestic product increased from 5.0% in 1960 to 17.5% in 2014 ([Centers for Medicare & Medicaid Services 2015c](#)) and is projected to increase to 19.6% by 2024 ([Centers for Medicare & Medicaid Services 2015b](#)). Prescription drugs

comprised 9.8% of U.S. spending for healthcare in 2014 ([Centers for Medicare & Medicaid Services 2015a](#)) and are projected to increase to 10.4% by 2024 ([Centers for Medicare & Medicaid Services 2015b](#)). The high costs of developing more effective and safer therapies, recently estimated at 1.4 billion US dollars per approved new compound ([DiMasi et al. 2016](#)), reflect an industry-wide 10.4% success rate from first-in-human studies

© The Author 2016. Published by Oxford University Press.

This is an Open Access article distributed under the terms of the Creative Commons Attribution-NonCommercial-NoDerivs license (<http://creativecommons.org/licenses/by-nc-nd/4.0/>), which permits non-commercial reproduction and distribution of the work, in any medium, provided the original work is not altered or transformed in any way, and that the work is properly cited. For commercial re-use, please contact [journals.permissions@oup.com](mailto:journals.permissions@oup.com)

to approval (Hay et al. 2014). Moreover, much of the failure occurs in Phase 2 (32% success rate) and Phase 3 (60% success rate) clinical trials (Hay et al. 2014), where costs are substantial (Paul et al. 2010). The main reasons for attrition are safety and lack of efficacy, which respectively accounted for 28% and 56% of molecules failing in Phase 2 or Phase 3 from 2011 to 2012 (Arrowsmith and Miller 2013). The ability to identify molecules with insufficient efficacy or safety issues prior to late-phase clinical development would reduce the costs and increase the rate of developing new therapeutics.

Over a decade ago, both industry (Colburn 2000) and regulators (Food and Drug Administration 2004) recognized that a new approach, taking advantage of advances in scientific and technical methods, was needed to improve efficiency along the path from laboratory concept to commercial product. The approval of 45 new drugs in 2015, the highest number approved since 53 were approved in 1996 (Mullard 2016), indicates that this new approach may be having an impact. One of the key elements in this new approach is the use of biomarkers, which are characteristics that are objectively measured and evaluated as indicators of normal biological processes, pathogenic processes, or pharmacologic responses to a therapeutic intervention (Biomarkers Definition Working Group 2001). In vivo imaging, when used appropriately, can provide biomarkers that supply information about biochemical, physiological, and anatomic processes. Information from imaging biomarkers in preclinical studies (i.e., target engagement, treatment response, safety, or mechanism of action) can have a critical impact on internal decision-making to help increase the odds of success for drugs taken into the clinic.

The ability of in vivo imaging to provide biomarkers without requiring surgery or euthanization to remove tissues also impacts the humane use of animals in pharmaceutical development. The guiding principles underpinning the humane use of animals in scientific research, introduced by Russell and Burch in 1959 (Russell and Burch 1959), are commonly known as the 3Rs, referring to replacement, reduction, and refinement in the use of animals. Replacement indicates changes in an experimental protocol to use alternative techniques (e.g., an in silico model) in place of animals. Reduction signifies approaches to obtain information from fewer animals or more information from the same number of animals, thereby reducing the number of animals needed to get information from an experiment. Refinement denotes modifications in the way experiments are carried out that minimize the actual or potential pain, distress, and other adverse effects experienced by the animals. Although in vivo imaging by definition requires animals and hence cannot replace animal use, it can both reduce and refine their use.

The use of in vivo imaging contributes to reduction in the number of animals used in preclinical drug development, because it allows repeated measurements to be made in the same animal. To longitudinally assess a treatment effect, other methods often require separate groups of animals to be euthanized so that measurements can be made for each study time point in each treatment group. Using in vivo imaging, because each animal can be evaluated at multiple time points, one group of animals can be used for all time points in each treatment group. By imaging animals prior to initiation of treatment, each animal serves as its own control. Hence, measurements at all time points for each animal using in vivo imaging not only reduce the number of animals, it also eliminates the impact of variability between animals in each time point group, thereby increasing statistical power. Moreover, animals can be assigned to treatment groups based on baseline

characteristics to minimize differences between treatment groups at baseline.

The noninvasive nature of in vivo imaging also provides a valuable tool for refinement, both when imaging is used to provide a biomarker or to facilitate other measurement methods. When imaging is used to provide a biomarker, it often replaces methods requiring removal of tissue, thereby minimizing pain and distress of the animals. In some instances where the imaging procedures are short in duration, minimal or no anesthesia is required further minimizing the animal's distress. Examples of the use of imaging to facilitate other measurement methods are the use of ultrasound imaging to guide the placement of a telemetry probe for blood pressure measurements (Campbell et al. 2008) and the use of magnetic resonance imaging (MRI) to guide intracranial delivery of therapeutics or for neurochemical sampling (Chen et al. 2015). In both instances, optimal placement is critical to acquire accurate reproducible data and improves animal quality of life by minimizing long-term adverse effects of inaccurate placement.

The methods used in preclinical studies are also available for clinical studies for most of the imaging modalities used in drug development. Consequently, the relationships between drug dose or exposure and target engagement, treatment response, or safety established in preclinical studies can be translated to studies in humans. The preclinical data provide a target for the magnitude of effects that should be observed in the clinical study if the drug is acting as it did in the preclinical model(s). Conversely, clinical imaging data can help to evaluate which animal model most closely reflects disease and the impact of treatment on the disease in humans.

## Imaging Modalities Used in Drug Development

Ultrasound imaging (also known as ultrasonography [US]) uses high frequency sound waves, outside the audible range of humans, to visualize structures of internal organs and their functions in both clinical and preclinical research and diagnostics (Cobbold 2007). Ultrasonic waves are delivered to tissues by an ultrasonic transducer, and the echoes that are reflected from tissues are detected via the same transducer. The time and strength of the echoes received by the probe, which are directly related to the position and density of tissues, are converted into pixels and displayed in an ultrasonic image. US is frequently used to see internal body structures such as tendons, muscles, joints, vessels, and internal organs and can assist in diagnosis of a disease and exclusion of suspicious pathology as well as assess response to treatment. In addition to the most commonly used B-mode cross-sectional structure image, US can also display the rate and direction of blood flow, the motion of tissue over time, and the stiffness of tissue as well as presence of specific molecular targets in blood vessels using microbubble contrast agents (Mulvagh et al. 2000). US is an economically efficient imaging approach and provides good contrast in most cardiovascular and abdominal tissues. Disadvantages of US include inter-operator variability and the difficulty of imaging tissues through bone or air.

Computed tomography (CT), also referred as a computerized axial tomography, is an X-ray-based imaging modality that produces detailed three-dimensional (3D) images (Romans 2011). X-rays penetrate samples and, depending on the properties of the sample, are attenuated as they traverse the sample to provide contrast. In a biological subject, bones attenuate X-rays the most, soft tissue next, and air the least. A CT scanner rotates opposing pairs of X-ray sources and detectors around the

subject, and a 3D image is reconstructed using a powerful computer. Bone, lung (air), and fatty tissues can be easily identified, allowing scientists to monitor disease progression and evaluate therapeutic responses *in vivo* over time noninvasively with high accuracy and repeatability. Due to poor inherent contrast between soft tissues, contrast materials such as intravenous iodinated contrast agents and orally administered barium sulfate are employed to better visualize heart, vasculature, brain, kidney, liver, gastrointestinal track, and tumors. In addition, since samples are subjected to a dose of ionizing radiation about 300 to 1000 times of conventional X-ray, for *in vivo* studies, the resulting increased risk of cancer and impact on proliferative tissues may need to be considered (Frush and Applegate 2004).

MRI is also commonly used to visualize tissues in animals and humans (Bushong 2003). MRI harnesses the magnetic properties, also known as spin, of the nucleus of hydrogen atoms contained in water and fat within tissues. When a strong magnetic field is applied to the body, the hydrogen spins act as little magnets and align with the direction of the magnetic field. A short radiofrequency pulse is applied to knock the hydrogen spins out of alignment. When the radio waves are turned off, the hydrogen spins realign, sending out radiofrequency signals. These signals provide information about the location and amount of the hydrogen spins in the body, which can be used to reconstruct a 3D image. In addition to water and fat content, the MRI signal can also be affected by the local microscopic magnetic environment, which varies from tissue to tissue and contributes to the excellent diverse soft tissue contrast in MRI. The MRI signal can be made sensitive to vascular flow (Srichai et al. 2009), to assess the dynamics and spatial distribution of blood flow within a vascular structure of interest, or diffusion (Le Bihan 2003), which informs on microscopic tissue architecture. MRI contrast agents, most commonly gadolinium-based, are also used to improve the visibility of internal body structures and vasculature and can provide functional information of specific tissues (O'Connor et al. 2012). In addition, functional MRI leverages blood flow and oxygenation changes during neuronal activation of different brain regions to visualize neural responses to external stimuli (Logothetis 2008). The length of time required for MRI acquisitions limits experimental throughput relative to optical, US, and CT.

Positron emission tomography (PET) and single-photon emission CT are nuclear imaging techniques that provide molecular information about tissue and organ function (Jaszczak and Coleman 1985; Wahl and Robert 2008). PET is based on detection of 2 photons emitted in opposite directions resulting from annihilation of a positron during the decay of a positron-emitting radioisotope.  $^{11}\text{C}$ ,  $^{18}\text{F}$ , and  $^{68}\text{Ga}$  are among the radioisotopes most frequently used to label molecules, which are commonly referred to as PET tracers because only a subphysiologic (trace) amount is needed to generate PET images. PET tracers designed to bind to specific proteins (often transmembrane receptors or enzymes) are also known as radioligands. After administration of a PET tracer into the body, a PET scanner measures its distribution by detecting the emitted photons in coincidence and reconstructing a 3D image. PET images can provide information about target occupancy, metabolism, and gene expression as well as bio-distribution of radiolabeled compounds. PET is often used in combination with CT or MRI to precisely co-register the PET images that convey molecular information with the anatomical location. Radiation exposure is inherent to the technology, limiting the number of repeat scans that can be performed on the same subject. The difficulty and cost of developing, producing, and transporting radiotracers are also limiting factors.

Optical imaging includes bioluminescence imaging (BLI), fluorescence imaging, and optical coherence tomography (OCT) (Weissleder et al. 2010). BLI is based on detection of visible light produced by reaction of a substrate (e.g., luciferin) with an enzyme (e.g., luciferase) expressed in genetically manipulated cells within living animals. Luciferases are found in many organisms, with firefly and click beetle luciferases most commonly used for *in vivo* imaging. Firefly luciferase catalyzes the light-producing reaction by oxidizing the substrate D-luciferin in the presence of oxygen and other cofactors such as ATP and magnesium (Wilson and Hastings 1998). The bioluminescence signal can be captured by an *in vivo* imaging system equipped with a very sensitive camera. As a genetic reporter, the luciferase gene can be incorporated into cells to track cell proliferation and trafficking, gene expression, biological pathway, and protein degradation as well as protein-protein interaction (Ozawa et al. 2013). BLI is sensitive, quantitative, cost effective, and has higher throughput than other imaging modalities; therefore it greatly increases the speed of preclinical research. However, translation of BLI into the clinic is limited by the requirement of genetic manipulation and attenuation of light from tissues.

*In vivo* fluorescence imaging also uses a sensitive camera to detect fluorescence emitted from fluorophores in small animals after exposure to light excitation. Exogenous near-infrared fluorescence probes can be designed to reflect different biological processes and tissue functions based on target specific binding, enzyme-specific activation, and tissue distribution (Ozawa et al. 2013). To detect fluorescence signals, subjects are administered with the probe, and external excitation light is delivered to the region of interest. The fluorophore absorbs an excitation photon and emits a longer wavelength photon, which is detected by a sensitive camera. Autofluorescence background, light scattering, and absorbance of tissues are inherent challenges in this technology. Current applications are mainly focused on small animals, with growing clinical applications in image-guided surgery (Allison 2016).

OCT is an optical imaging technique used to capture micrometer-resolution 3D images just below the surface in biological tissues. OCT applies an echo technique, similar to US, using light instead of sound to detect the reflection of light from an object. Light is split into 2 paths: a reference mirror and the tissue. A small portion of the light that reflects from subsurface tissue is combined with the reference light from the reference arm, resulting in an interference pattern, which contains the spatial dimensions and location of structures of tissue. Light scattering from opaque biological tissues limits the depth of OCT to 1 to 2 mm. Although it is used in preclinical studies, its primary use is in the clinic to detect high-resolution structures of the eye to assess axonal integrity in multiple sclerosis, macular degeneration, progression of glaucoma, and diabetic macular edema (Kostanyan et al. 2015).

## Use for Target Engagement

Teams in the pharmaceutical industry focused on discovery and development of drugs for targets in the central nervous system have long recognized the value of target engagement for increasing confidence, guiding dose selection, and reducing risk at key stages of the discovery and development process (Honer et al. 2014). PET provides a noninvasive, quantitative measure of target (e.g., receptor, enzyme, ion channel) distribution in tissues using a radioligand with high affinity and selectivity for the specific target of interest. Target binding site

density (location and amount) is assessed by kinetic modeling of PET tracer distribution over time in specific regions of interest (i.e., previously defined anatomic regions that may be known to be target-rich or target-deficient based on in vitro studies) derived from dynamic PET data and from the PET tracer concentration in arterially sampled blood (Carson 2005). PET target engagement studies are typically conducted by following a baseline PET scan, which uses only the radioligand to assess baseline target density, with a second scan in the same animal where the radioligand is administered after a test drug. In target-rich regions, the amount of target measured by the radioligand is lower in the PET scan after test drug administration compared to the baseline PET scan if the test drug competes with the radioligand for the target (Cunningham et al. 2004). Assessment of the change in amount of target in specific regions of interest before and after drug provides a quantitative assessment of target occupancy (Innis et al. 2007). Each pair of baseline and post-drug PET scans provides one value for occupancy at the exposure (dose) of the test drug. A dose- or exposure-to-occupancy relationship is obtained from a group of subjects receiving baseline and post-drug PET scans at various drug exposures and/or administering the radioligand at different times post-drug administration. The use of PET to determine such exposure-to-occupancy relationships has a significant impact on reduction and refinement, because the same animal can be evaluated and recovered in drug occupancy PET studies multiple times. Previously, such relationships were determined from terminal animal studies where drug occupancy is assessed by ex vivo measurement of radioligand binding.

A recent example of the use of PET for evaluating target engagement is provided by [<sup>11</sup>C]MK-8193, which is a PDE10A-specific PET tracer (Cox et al. 2015). Inhibition of PDE10A, which enhances striatal output by increasing activity in the cGMP and cAMP signaling pathways (Siuciak et al. 2006), is a target being developed for the potential to provide efficacy on positive, cognitive, and negative symptoms of schizophrenia (Jan and Jacob 2011). Studies in rhesus monkeys (Figure 1) demonstrate that highest radioligand uptake is in the striatum, with very low retention in all other brain regions, and that THPP-1, a potent PDE10A inhibitor (Smith et al. 2013), engaged with the molecular drug target. Further studies in rhesus monkeys and rats (Hostetler et al. 2015) demonstrated similar target occupancy

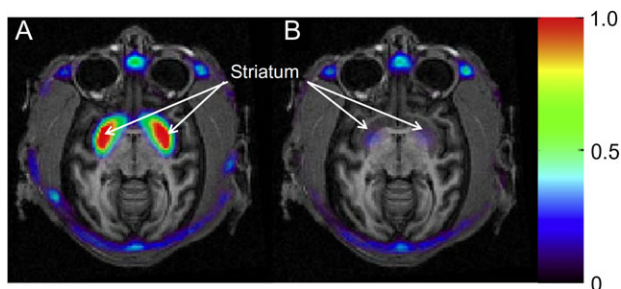


**Figure 1.** Summed PET images (30–90 min) of [<sup>11</sup>C] MK-8193 in rhesus monkey brain overlaid on MRI under baseline conditions (A) and after administration of THPP-1 (B). The baseline PET study shows high tracer retention (red color) in the striatum. Tracer binding in the striatum is blocked after administration of THPP-1. Scale is in SUV (standardized uptake value).

[Reprinted from Cox CD, Hostetler ED, Flores BA, Evelhoch JL, Fan H, Gantert L, Holahan M, Eng W, Joshi A, McGaughey. 2015. Discovery of [<sup>11</sup>C]MK-8193 as a PET tracer to measure target engagement of phosphodiesterase 10A (PDE10A) inhibitors, *Bioorganic Medical Chemistry Letters*, with permission from Elsevier.]

curves for THPP-1 in both species (Figure 2), although this is not always the case.

Combination of target occupancy curves with efficacy data from preclinical studies can establish a suitable range of exposures for testing in clinical studies and ensure that target engagement is sufficient when the clinical proof of concept trial is conducted. If the proof of concept trial is positive, the dose-occupancy information can be used to maximize efficacy while minimizing associated side effects. On the other hand, if sufficient target occupancy levels are obtained and the outcome of the proof of concept trial is negative, a clear decision can be made that the mechanistic hypothesis for the therapeutic approach is invalid. The development of neurokinin 1 (NK1) receptor antagonist provides a good example of both cases. When evaluated in clinical trials for treatment of depression (Keller et al. 2006) or anxiety (Michelson et al. 2013), the NK1 antagonist L-759274 showed no statistically significant differences from placebo. Because clinical PET receptor occupancy studies with [<sup>18</sup>F]SPARQ (Keller et al. 2006) indicated that the doses used in these studies achieved very high occupancies that effectively blocked the NK1 receptor system in the brain continuously throughout the study period, confidence that the proof of concept was adequately tested led to the decision to stop pursuing those indications. However, for prevention of acute and delayed chemotherapy-induced nausea and vomiting, aprepitant, a selective NK1 antagonist, was effective (Hargreaves et al. 2011). In this case, PET studies were used to pick the lowest dose that demonstrated full central nervous system target engagement, thereby optimizing the therapeutic window and minimizing potential drug-drug interactions associated with complex drug regimens used in oncology.

## Use for Treatment Response

Therapeutic efficacy is often linked to changes in tissue gene expression, biochemistry, physiology, and/or morphology in response to the drug. These pharmacodynamic (PD) effects may follow a dose-response relationship and may precede a therapeutic benefit. The objective measurement of these PD effects can lead to biomarker candidates with preclinical and clinical applicability (Frank and Hargreaves 2003). Expression of pharmacological activity commensurate with target engagement increases confidence that the hypothesized therapeutic mechanism is adequately being tested (Morgan et al. 2012).

Biomarkers may be based on the PD effect of compounds on blood chemistry, making repeat measurements practical. For instance, the dose-dependent effect of statins on HMG-CoA reductase is readily reflected by decreases in circulating LDL cholesterol (Nissen et al. 2005). In some instances, however, there may not be a systemic measure of a PD effect at the site of action, and the molecular target may be constrained to a specific deep tissue or organ system. In those situations, it may be necessary to assess the PD effect at the site of action. The direct measurement of a biomarker in tissue may require necropsy in the case of animal models or biopsy in clinical cases. Imaging allows noninvasive and longitudinal measurements of tissue properties in vivo. The following 2 examples show how imaging has a direct impact on the principle of reduction in animal research, specifically in the context of the measurement of PD effects.

Genetically engineered mouse models are crucial for testing of candidate targeted therapeutic compounds. Genetically engineered mouse models are often difficult to produce and expensive, and their availability may be limited due to complex

breeding. In the case of the K-ras<sup>LSL-G12D</sup> and K-ras<sup>LSL-G12D/p53LSL-R270H</sup> models (Olive et al. 2004), Adeno-Cre viral activation leads to the development of lung tumors. Tumors may develop at a highly variable rate, deep in the body, making size measurements that rely on traditional caliper techniques impossible in vivo. Necropsies must therefore be used to monitor tumor progression and regression due to pharmacologic intervention. Haines et al. (2009) demonstrated the use of micro x-ray CT to perform volumetric lung tumor measurements in K-ras<sup>LSL-G12D</sup> and K-ras<sup>LSL-G12D/p53LSL-R270H</sup> mice, showing that this novel technique can be used to monitor both tumor progression and dose-dependent response to treatment with Erlotinib (see Figure 3). This high-throughput micro x-ray CT imaging approach provided real-time in vivo quantitative baseline evaluation of tumor burden of all mice in the study across several time points after viral induction and enabled same-subject monitoring of tumor inhibition.

Abnormally highly expressed molecular cell surface markers are often a distinguishing feature of malignancies. Imaging of tumor molecular cell surface targets using PET radioligands is feasible in animal models and in the clinic. Epidermal growth factor receptor family member ErbB-2 (HER-2) is a cell surface

protein with a prominent signaling role in a significant percentage of breast cancers (Slamon et al. 1987). HER-2 is a client protein of the molecular chaperone heat shock protein 90 (HSP90), which confers stability to HER-2, making HSP90 a potential therapeutic target (Banerji 2009). Smith-Jones et al. (2004) demonstrated that HSP90 inhibition could be monitored in a murine xenograft model by PET imaging of HER-2 expression using a <sup>68</sup>Ga labeled F(ab')<sub>2</sub> radiotracer. Noninvasive PET imaging of HER-2 expression enabled the in vivo exploration of dynamic loss and recovery of tumor HER-2 expression following HSP90 inhibition. Furthermore, PET imaging enabled time-dependent measurements in vivo in the same subject (see Figure 4), minimizing the number of animals required by allowing pair-wise comparisons of changes in the HER-2 PET signal due to HSP90 inhibition, which increased the statistical power. Based on these findings, it was hypothesized that PET imaging of HER-2 could be used as a downstream PD measure of HSP90 inhibition in a clinical setting. The anti-HER2 antibody Trastuzumab, labeled with the <sup>89</sup>Zr PET radioisotope, was subsequently used to confirm the clinical target inhibition of HSP90 in metastatic breast cancer patients (Gaykema et al. 2014).

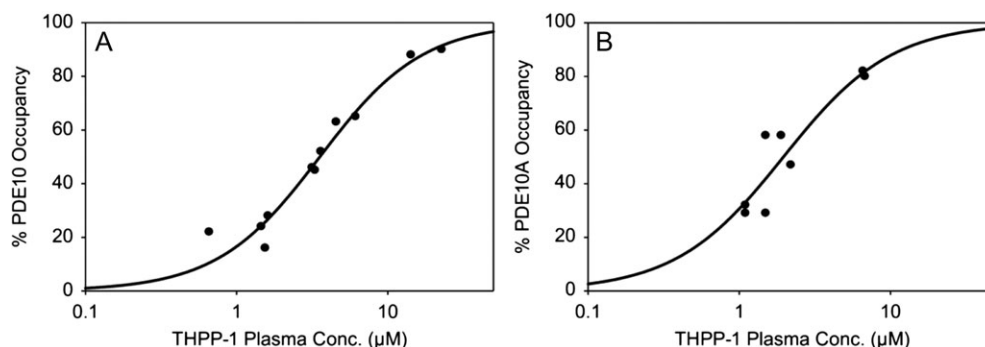


**Figure 2.** Plasma concentration vs PDE10A enzyme occupancy relationship in a monkey brain and b rat brain for THPP-1 as determined by PET studies with [<sup>11</sup>C]MK-8193. [Reprinted from Hostetler ED, Fan H, Joshi AD, Zeng Z, Eng W, Gantert L, Holahan M, Meng X, Miller P, O'Malley S, Purcell M, Riffel K, Salinas C, Williams M, Ma B, Buist N, Smith SM, Coleman PJ, Cox CD, Flores BA, Raheem IT, Cook JJ, Evelhoch JL. 2015. Preclinical characterization of the phosphodiesterase 10A PET tracer [<sup>11</sup>C]MK-8193, Mol Imaging Biol, with permission of Springer.]

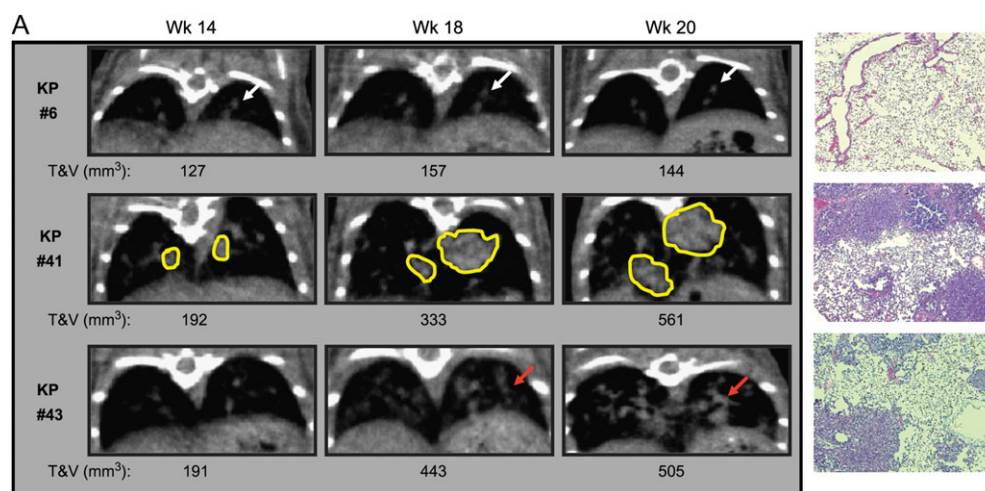


**Figure 3.** Visualization of lung tumor development in K-ras<sup>LSL-G12D</sup>/p53LSL-R270H (KP) models. Panel 1: Example of CT images of a control KP mouse with no tumor and H&E stain. Panel 2: Example of CT images of a KP mouse infected with a high dose of Adeno-Cre virus with isolated lung tumors and H&E stain. Panel 3: Example of CT images of a KP mouse infected with a high dose of Adeno-Cre virus with small multifocal tumors and H&E stain. [Reprinted from Haines BB, Bettano KA, Chenard M, Sevilla RS, Ware C, Angagaw MH, Winkelmann CT, Tong C, Reilly JF, Sur C, Zhang W. 2009. A quantitative volumetric micro-computed tomography method to analyze lung tumors in genetically engineered mouse models, Neoplasia, with permission from Elsevier.]

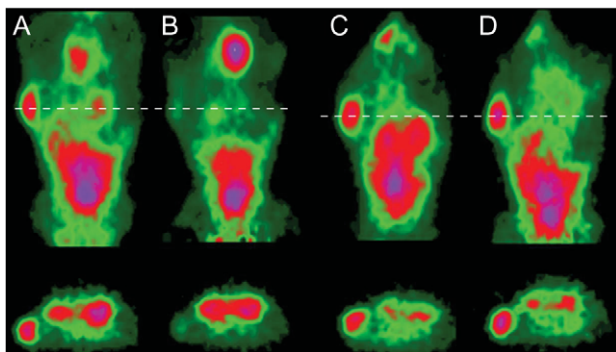


**Figure 4.** MicroPET images (coronal slice and transverse slice through tumor and kidneys) of 2 different nude mice with single BT-474 tumors. (A) A mouse at 3 hours after injection with  $^{68}\text{Ga}$ -DCHF and before 17-allylaminogeldanamycin (17-AAG) treatment. (B) The same mouse after it had received  $3 \times 50\text{ mg/kg}$  of 17-AAG and rescanned 24 hours later. (C,D) Comparable images of a control mouse 3 hours after 1 dose of  $^{68}\text{Ga}$ -DCHF (C) and after a second dose 24 hours later (D). [Reprinted from Smith-Jones PM, Solit DB, Akhurst T, Afroz F, Rosen N, Larson SM. 2004. Imaging the pharmacodynamics of HER2 degradation in response to Hsp90 inhibitors. *Nat Biotechnol*, by permission from Macmillan Publishers Ltd: NATURE BIOTECHNOLOGY.]

### Use for Safety

Multiple imaging modalities have the ability to assess potential safety-related treatment effects in drug development. Many preclinical imaging protocols are adapted from established clinical protocols or published animal experiments to not only ensure the translatability of the techniques for assessment, but also to further ensure that accepted and reliable methodologies are being used. First, imaging can be a powerful de-risking tool, where direct or indirect effects due to treatment are measured. While de-risking studies appear similar to PD or efficacy studies, the treated animals are normal, healthy animals such that any undesired observed effects can be attributed solely to treatment effects and represent safety risks. As such, imaging typically answers de-risking questions involving the presence or absence of an effect, dose dependence of the effect, and the potential reversibility of this effect. Second, imaging can be used to generate new, noninvasive safety biomarkers. The presence of a direct or indirect effect can be used as a biomarker if the effect is sensitive and specific to the treatment, reliable, and shows dose dependence. To begin developing these safety biomarkers, animals must be treated with a molecule known to induce a detectable effect and monitored with an appropriate imaging modality.

MRI, CT, and US are more routinely accessible and available as preclinical imaging modalities in assessing safety-related treatment effects. 3D techniques such as MRI and CT allow for accurate volume measurements, which can serve as a surrogate measure for organ weight. As mentioned earlier, MRI provides excellent soft tissue contrast and can consequently provide volume measurements of soft tissue, such as in brain regions. Posaconazole IV Solution (POS IV), a potent, selective triazole antifungal approved for use in adult patients, was found to enlarge the lateral ventricles of the brain in 5 of 8 juvenile preweaning dogs during necropsy at the conclusion of a 6-week dosing period. To determine if this was a treatment effect to support the administration of POS IV in children 2 years and older and in adults 18 years and older, Hines et al. (2015) used MRI to measure the volumes of dog brain ventricles before and during 12 weeks of treatment with POS IV. In a

study using 36 juvenile and 16 adult dogs, POS IV had no effect on ventricle volume at any timepoint during dosing in either the adult or the juvenile dogs. In this study, the ability to classify the animals' ventricle size at baseline (Figure 5) so that animals that were obviously different from the rest of the cohort were not included in a single group, which would skew the results of the study, and to distribute the sizes of ventricles between groups as best as possible was critical to rigorous evaluation of a potential treatment effect. Two-dimensional US and 3-dimensional CT techniques can similarly assess area or volume, respectively, to equally distribute effects between treatment groups. CT imaging is used routinely for bone assessment, as metals such as calcium increase X-ray attenuation. As such, bone mineral density measurements can quantify the amount of bone loss or gain due to treatment (Williams et al. 2013). CT has also been used to evaluate developing bone in response to reproductive toxicants (Wise et al. 2013; Wise et al. 2010). Lastly, US is a mobile and rapid measurement that can provide high-throughput assessment compared to MRI and CT. Similar to MRI, US can also assess soft tissues easily. Preclinical cardiac US (echocardiography) is highly translatable to the clinic for cardiac de-risking, for example, in providing functional contractility or blood flow information. Finally, as MRI, US, and CT imaging can be used to monitor treatment effects during studies, recovery of these effects can also be monitored to determine the permanence of treatment or return animals to colonies, for example, thereby promoting the 3Rs. For example, Lenhard et al. (2016) applied dynamic contrast-enhanced MRI to detect changes in hepatobiliary transporter function as a result of amiodarone-induced hepatic phospholipidosis before, during, and 2 weeks after cessation of amiodarone treatment. The calculated rates of contrast agent wash-out, which is dependent on efflux transporter function, decreased with treatment and fully recovered after cessation of treatment. These results demonstrated the ability to monitor drug-induced liver injury using novel clinically translatable biomarkers in a preclinical setting.

Additionally, PET can be used for noninvasive safety assessment, although this modality is less routinely used due to the increased logistics involved with radioisotopes, radiochemistry, and sensitive timing. Similarly, optical imaging can be used for safety assessment applications but is often limited by its depth-dependent nature. However, OCT has recently been successfully applied to address ophthalmic toxicity (Fielden et al. 2015) and has the additional benefit of being directly translatable to the clinic.

### Use for Mechanism of Action

Mechanism of action (MoA) can be defined as the biochemical interaction through which a drug produces its effect. With imaging, this can be measured from the cell level to organ level and all the way to the animal level. Use of reporter genes has allowed researchers to probe the MoA of receptors via signal transduction cascades at the cell level. These assays are typically refined in vitro and then translated to the animal level using transgenic mice or simply using tumor-bearing mice. In one study, reporter gene imaging was used to monitor activation of the Erb2/Her2/neu pathway during radiotherapy (Wolf et al. 2011). Using a split luciferase model, they were able to develop and refine a method based on the MoA of Erb2 signal transduction that could be used to screen compounds that interfere with Erb2 activation in cell culture. The same cells were then used to create tumor-bearing mice that could be

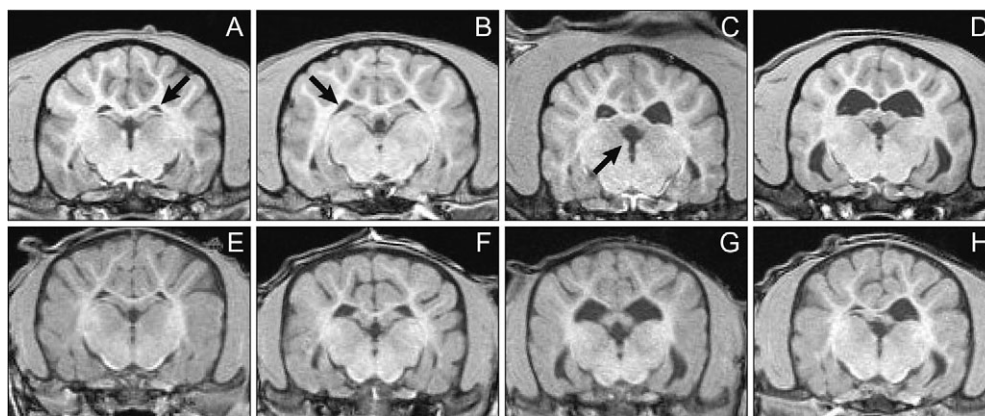


**Figure 5.** Examples of small (A), medium (B), large (C), and very-large (D) lateral brain ventricles in the adult dogs (top) and juvenile dogs (bottom) at baseline MRI images. No very large ventricles were found in the juvenile group based on adult dog experience, so only small (E), medium (F), and large (G) juvenile lateral ventricles are shown along with a small right and a large left lateral ventricle to demonstrate an example of asymmetry seen in this study (H). While G of the juvenile dogs appears similar to D of the adult dogs, baseline assessment was based on 3D visualization, whereas the images in this 2D figure were chosen to show the ventricles at a similar cross section of all animals. Qualitative assessment of the ventricle size and distribution of differently sized ventricles between groups was warranted as not to skew group means for the adult and juvenile dogs' treatment groups. Arrows point to the left lateral, right lateral, and third ventricle in A, B, and C, respectively. [Reprinted from Hines CDG, Song X, Kuruville S, Farris G, Markgraf CG. 2015. Magnetic resonance imaging assessment of the ventricular system in the brains of adult and juvenile beagle dogs treated with posaconazole IV Solution, *J Pharmacol Toxicol Methods*, with permission from Elsevier.]

used to monitor Erb2 activation. Since the same animals could be monitored before, during, and after treatment, the number of animals needed to screen potential drug candidates was reduced.

More specific modes of action of a disorder can be visualized through the use of reporter genes, which then can be used to determine dose response, dose selection, and needed drug levels to produce MoA and therapeutic response. Polycythemia vera is a disorder in which a somatic mutation of the gene encoding JAK2 causes myeloproliferation (James et al. 2005). The same mode of action can be recapitulated in mice when bone marrow expressing the mutation is used to reconstitute irradiated mice (Wernig et al. 2006). A luciferase-based model was developed in which cells expressing the mutation could be monitored using in vivo BLI (Ma et al. 2009). This made it possible to examine the kinetics of disease regression and resurgence noninvasively. Since the same animals were scanned at multiple time points, the numbers of animals for the study were reduced. The results led to the development of an intermittent dosing schedule that achieved significant reductions in both erythroid and myeloid populations with minimal impact on lymphoid cells. This provided a rationale for the use of non-continuous treatment to provide optimal therapy for PV patients (Kraus et al. 2012).

## Conclusions

Improved ability to identify molecules with insufficient efficacy or safety issues prior to late-phase clinical development is needed to reduce the costs and increase the rate of developing new therapeutics. In vivo imaging can provide information in preclinical studies (i.e., target engagement, treatment response, safety, or mechanism of action) that has a critical impact on internal decision-making to help increase the odds of success for drugs taken into the clinic.

Most of the imaging modalities used in preclinical studies translate to the clinic. The number of preclinical subjects required for a study is reduced, because in vivo imaging does not require surgery or euthanasia to obtain the desired

information. The number of subjects needed for the evaluation of treatment effects in animal models is further reduced by the ability of imaging to provide quantitative intra-subject comparisons that enhance statistical power. The noninvasive nature of in vivo imaging can also help to alleviate or minimize potential for pain or distress in research animals.

## Acknowledgments

The authors thank Drs. Eric Hostetler, Cyrille Sur, Richard Kennan, Michael Klimas, and Joseph DeGeorge for their insightful feedback.

## References

- Allison RR. 2016. Fluorescence guided resection (FGR): a primer for oncology. *Photodiagnosis Photodyn Ther* 13:73–80.
- Arrowsmith J, Miller P. 2013. Trial watch: phase II and phase III attrition rates 2011–2012. *Nat Rev Drug Discov* 12(8):569.
- Banerji U. 2009. Heat shock protein 90 as a drug target: some like it hot. *Clin Cancer Res* 15(1):9–14.
- Biomarkers Definitions Working Group. 2001. Biomarkers and surrogate endpoints: preferred definitions and conceptual framework. *Clin Pharmacol Ther* 69(3):89–95.
- Bushong SC. 2003. *Magnetic Resonance Imaging: Physical and Biological Principles*. St. Louis, MO: Mosby.
- Campbell BR, Bunzel MM, Zhang C, Shen X, Ahn C, Johnson CV, Cai T-Q, Walker M. 2008. A novel approach to telemetry blood pressure probe placement in mice using high frequency micro-ultrasound guided surgery. *FASEB J* 22(2 Supplement):11.
- Carson RE. 2005. Tracer kinetic modeling in PET. In: Bailey DL, Townsend DW, Valk PE, Maisey MN, eds. *Positron Emission Tomography: Basic Sciences*. London: Springer London. p. 127–159.
- Centers for Medicare & Medicaid Services. 2015a National health expenditures by type of service and source of funds: calendar years 1960–2014 [Internet]. Available online <https://www.cms.gov/Research-Statistics-Data-and-Systems/Statistics-Trends-and-Reports/NationalHealthExpendData/Downloads/NHE2014.zip>, accessed on November 5, 2015.

- Centers for Medicare & Medicaid Services. 2015b NHE projections 2014–2024 - Tables [Internet]. Available online <https://www.cms.gov/Research-Statistics-Data-and-Systems/Statistics-Trends-and-Reports/NationalHealthExpendData/Downloads/Proj2014tables.zip>, accessed on November 5, 2015.
- Centers for Medicare & Medicaid Services. 2015c NHE summary including share of GDP, CY 1960–2014 [Internet]. Available online <https://www.cms.gov/Research-Statistics-Data-and-Systems/Statistics-Trends-and-Reports/NationalHealthExpendData/Downloads/NHEGDP14.zip>, accessed on November 5, 2015.
- Chen A, Hines C, Dogdas B, Bone A, Lodge K, O'Malley S, Connolly B, Winkelmann CT, Bagchi A, Lubbers LS, Uslaner JM, Johnson C, Renger J, Zariwala HA. Targeting of deep-brain structures in nonhuman primates using MR and CT Images. 2015. p. 94152K–94152K-9.
- Cobbold RSC. 2007. Foundations of biomedical ultrasound. New York: Oxford University Press, Inc.
- Colburn WA. 2000. Optimizing the use of biomarkers, surrogate endpoints, and clinical endpoints for more efficient drug development. *J Clin Pharmacol* 40(12 Pt 2):1419–1427.
- Cox CD, Hostetler ED, Flores BA, Evelhoch JL, Fan H, Gantert L, Holahan M, Eng W, Joshi A, McGaughey G, Meng X, Purcell M, Raheem IT, Riffel K, Yan Y, Renger JJ, Smith SM, Coleman PJ. 2015. Discovery of [<sup>11</sup>C]MK-8193 as a PET tracer to measure target engagement of phosphodiesterase 10A (PDE10A) inhibitors. *Bioorg Med Chem Lett* 25(21):4893–4898.
- Cunningham VJ, Gunn RN, Matthews JC. 2004. Quantification in positron emission tomography for research in pharmacology and drug development. *Nucl Med Commun* 25(7):643–646.
- DiMasi JA, Grabowski HG, Hansen RW. 2016. Innovation in the pharmaceutical industry: new estimates of R&D costs. *J Health Econ* 47:20–33.
- Fielden MR, Werner J, Jamison JA, Coppi A, Hickman D, Dunn RT 2nd, Trueblood E, Zhou L, Afshari CA, Lightfoot-Dunn R. 2015. Retinal toxicity induced by a novel beta-secretase inhibitor in the Sprague-Dawley rat. *Toxicol Pathol* 43(4):581–592.
- Food and Drug Administration. 2004. Innovation or stagnation: challenge and opportunity on the critical path to new medical products [Internet]. Available online <http://www.fda.gov/ScienceResearch/SpecialTopics/CriticalPathInitiative/CriticalPathOpportunitiesReports/ucm077262.htm>, accessed on March 27, 2004.
- Frank R, Hargreaves R. 2003. Clinical biomarkers in drug discovery and development. *Nat Rev Drug Discov* 2(7):566–580.
- Frush DP, Applegate K. 2004. Computed tomography and radiation: understanding the issues. *J Am Coll Radiol* 1(2):113–119.
- Gaykema SB, Schroder CP, Vitfell-Rasmussen J, Chua S, Oude Munnink TH, Brouwers AH, Bongaerts AH, Akimov M, Fernandez-Ibarra C, Lub-de Hooge MN, de Vries EG, Swanton C, Banerji U. 2014. <sup>89</sup>Zr-Trastuzumab and <sup>89</sup>Zr-bevacizumab PET to evaluate the effect of the HSP90 inhibitor NVP-AUY922 in metastatic breast cancer patients. *Clin Cancer Res* 20(15):3945–3954.
- Haines BB, Bettano KA, Chenard M, Sevilla RS, Ware C, Angagaw MH, Winkelmann CT, Tong C, Reilly JF, Sur C, Zhang W. 2009. A quantitative volumetric micro-computed tomography method to analyze lung tumors in genetically engineered mouse models. *Neoplasia* 11(1):39–47.
- Hargreaves R, Ferreira JC, Hughes D, Brands J, Hale J, Mattson B, Mills S. 2011. Development of aprepitant, the first neurokinin-1 receptor antagonist for the prevention of chemotherapy-induced nausea and vomiting. *Ann N Y Acad Sci* 1222:40–48.
- Hay M, Thomas DW, Craighead JL, Economides C, Rosenthal J. 2014. Clinical development success rates for investigational drugs. *Nat Biotechnol* 32(1):40–51.
- Hines CD, Song X, Kuruvilla S, Farris G, Markgraf CG. 2015. Magnetic resonance imaging assessment of the ventricular system in the brains of adult and juvenile beagle dogs treated with posaconazole IV solution. *J Pharmacol Toxicol Methods* 76:55–64.
- Honer M, Gobbi L, Martarello L, Comley RA. 2014. Radioligand development for molecular imaging of the central nervous system with positron emission tomography. *Drug Discov Today* 19(12):1936–1944.
- Hostetler ED, Fan H, Joshi AD, Zeng Z, Eng W, Gantert L, Holahan M, Meng X, Miller P, O'Malley S, Purcell M, Riffel K, Salinas C, Williams M, Ma B, Buist N, Smith SM, Coleman PJ, Cox CD, Flores BA, Raheem IT, Cook JJ, Evelhoch JL. 2016. Preclinical characterization of the phosphodiesterase 10A PET tracer [<sup>11</sup>C]MK-8193. *Mol Imaging Biol*. 18:579–587.
- Innis RB, Cunningham VJ, Delforge J, Fujita M, Gjedde A, Gunn RN, Holden J, Houle S, Huang SC, Ichise M, Iida H, Ito H, Kimura Y, Koeppe RA, Knudsen GM, Knuuti J, Lammertsma AA, Laruelle M, Logan J, Maguire RP, Mintun MA, Morris ED, Parsey R, Price JC, Slifstein M, Sossi V, Suhara T, Votaw JR, Wong DF, Carson RE. 2007. Consensus nomenclature for in vivo imaging of reversibly binding radioligands. *J Cereb Blood Flow Metab* 27(9):1533–1539.
- James C, Ugo V, Le Couedic J-P, Staerk J, Delhommeau F, Lacout C, Garcon L, Raslova H, Berger R, Bennaceur-Griscelli A, Villeval JL, Constantinescu SN, Casadevall N, Vainchenker W. 2005. A unique clonal JAK2 mutation leading to constitutive signalling causes polycythaemia vera. *Nature* 434(7037):1144–1148.
- Jan K, Jacob N. 2011. PDE10A inhibitors: novel therapeutic drugs for schizophrenia. *Curr Pharm Des* 17(2):137–150.
- Jaszczak RJ, Coleman RE. 1985. Single photon emission computed tomography (SPECT). Principles and instrumentation. *Invest Radiol* 20(9):897–910.
- Keller M, Montgomery S, Ball W, Morrison M, Snavely D, Liu G, Hargreaves R, Hietala J, Lines C, Beebe K, Reines S. 2006. Lack of efficacy of the substance p (neurokinin1 receptor) antagonist aprepitant in the treatment of major depressive disorder. *Biol Psychiatry* 59(3):216–223.
- Kostanyan T, Wollstein G, Schuman JS. 2015. New developments in optical coherence tomography. *Curr Opin Ophthalmol* 26(2):110–115.
- Kraus M, Wang Y, Aleksandrowicz D, Bachman E, Szewczak AA, Walker D, Xu L, Bouthillette M, Childers KM, Dolinski B, Haidle AM, Kopinja J, Lee L, Lim J, Little KD, Ma Y, Mathur A, Mo J-R, O'Hare E, Otte RD, Taoka BM, Wang W, Yin H, Zabierek AA, Zhang W, Zhao S, Zhu J, Young JR, Marshall CG. 2012. Efficacious intermittent dosing of a novel JAK2 inhibitor in mouse models of polycythemia vera. *PLoS One* 7(5):e37207.
- Le Bihan D. 2003. Looking into the functional architecture of the brain with diffusion MRI. *Nat Rev Neurosci* 4(6):469–480.
- Lenhard SC, Lev M, Webster LO, Peterson RA, Goulbourne CN, Miller RT, Jucker BM. 2016. Hepatic phospholipidosis is associated with altered hepatobiliary function as assessed by gadoxetate dynamic contrast-enhanced magnetic resonance imaging. *Toxicol Pathol* 44(1):51–60.



- Logothetis NK. 2008. What we can do and what we cannot do with fMRI. *Nature* 453(7197):869–878.
- Ma Y, Zhao S, Zhu J, Bettano KA, Qu X, Marshall CG, Young JR, Kohl NE, Scott ML, Zhang W, Wang Y. 2009. Real-time bioluminescence imaging of polycythemia vera development in mice. *Biochim Biophys Acta* 1792(11):1073–1079.
- Michelson D, Hargreaves R, Alexander R, Ceasay P, Hietala J, Lines C, Reines S. 2013. Lack of efficacy of L-759274, a novel neurokinin 1 (substance P) receptor antagonist, for the treatment of generalized anxiety disorder. *Int J Neuropsychopharmacol* 16(1):1–11.
- Morgan P, Van Der Graaf PH, Arrowsmith J, Feltner DE, Drummond KS, Wegner CD, Street SD. 2012. Can the flow of medicines be improved? Fundamental pharmacokinetic and pharmacological principles toward improving Phase II survival. *Drug Discov Today* 17(9–10):419–424.
- Mullard A. 2016. 2015 FDA drug approvals. *Nat Rev Drug Discov* 15(2):73–76.
- Mulvagh SL, DeMaria AN, Feinstein SB, Burns PN, Kaul S, Miller JG, Monaghan M, Porter TR, Shaw LJ, Villanueva FS. 2000. Contrast echocardiography: current and future applications. *J Am Soc Echocardiogr* 13(4):331–342.
- Nissen SE, Tuzcu EM, Schoenhagen P, Crowe T, Sasiela WJ, Tsai J, Orazem J, Magorien RD, O’Shaughnessy C, Ganz P. 2005. Statin therapy, LDL cholesterol, C-reactive protein, and coronary artery disease. *N Engl J Med* 352(1):29–38.
- O’Connor JP, Jackson A, Parker GJ, Roberts C, Jayson GC. 2012. Dynamic contrast-enhanced MRI in clinical trials of antivasculic therapies. *Nat Rev Clin Oncol* 9(3):167–177.
- Olive KP, Tuveson DA, Ruhe ZC, Yin B, Willis NA, Bronson RT, Crowley D, Jacks T. 2004. Mutant p53 gain of function in two mouse models of Li-Fraumeni syndrome. *Cell* 119(6):847–860.
- Ozawa T, Yoshimura H, Kim SB. 2013. Advances in fluorescence and bioluminescence imaging. *Anal Chem* 85(2):590–609.
- Paul SM, Mytelka DS, Dunwiddie CT, Persinger CC, Munos BH, Lindborg SR, Schacht AL. 2010. How to improve R&D productivity: the pharmaceutical industry’s grand challenge. *Nat Rev Drug Discov* 9(3):203–214.
- Romans LE. 2011. *Computed Tomography for Technologists: A Comprehensive Text*. Philadelphia: Wolters Kluwer Health / Lippincott Williams & Wilkins.
- Russell WMS, Burch RL. 1959. *The Principles of Humane Experimental Technique*. London: Methuen & Co. Ltd.
- Siuciak JA, Chapin DS, Harms JF, Lebel LA, McCarthy SA, Chambers L, Shrikhande A, Wong S, Menniti FS, Schmidt CJ. 2006. Inhibition of the striatum-enriched phosphodiesterase PDE10A: a novel approach to the treatment of psychosis. *Neuropharmacology* 51(2):386–396.
- Slamon DJ, Clark GM, Wong SG, Levin WJ, Ullrich A, McGuire WL. 1987. Human breast cancer: correlation of relapse and survival with amplification of the HER-2/neu oncogene. *Science* 235(4785):177–182.
- Smith SM, Uslander JM, Cox CD, Huszar SL, Cannon CE, Vardigan JD, Eddins D, Toolan DM, Kandebo M, Yao L, Raheem IT, Schreier JD, Breslin MJ, Coleman PJ, Renger JJ. 2013. The novel phosphodiesterase 10A inhibitor THPP-1 has antipsychotic-like effects in rat and improves cognition in rat and rhesus monkey. *Neuropharmacology* 64:215–223.
- Smith-Jones PM, Solit DB, Akhurst T, Afroze F, Rosen N, Larson SM. 2004. Imaging the pharmacodynamics of HER2 degradation in response to Hsp90 inhibitors. *Nat Biotechnol* 22(6):701–706.
- Srichai MB, Lim RP, Wong S, Lee VS. 2009. Cardiovascular applications of phase-contrast MRI. *AJR Am J Roentgenol* 192(3):662–675.
- Wahl RLB, Robert SB. 2008. *Principles and Practice of PET and PET/CT*. Philadelphia: Lippincott Williams & Wilkins.
- Weissleder R, Ross BD, Rehemtulla A, Gambhir SS. 2010. *Molecular Imaging Principle and Practices*. Shelton, CT: People’s Medical Publishing House-USA.
- Wernig G, Mercher T, Okabe R, Levine RL, Lee BH, Gilliland DG. 2006. Expression of Jak2V617F causes a polycythemia vera-like disease with associated myelofibrosis in a murine bone marrow transplant model. *Blood* 107(11):4274–4281.
- Williams DS, McCracken PJ, Purcell M, Pickarski M, Mathers PD, Savitz AT, Szumiloski J, Jayakar RY, Somayajula S, Krause S, Brown K, Winkelmann CT, Scott BB, Cook L, Motzel SL, Hargreaves R, Evelhoch JL, Cabal A, Dardzinski BJ, Hangartner TN, Duong LT. 2013. Effect of odanacatib on bone turnover markers, bone density and geometry of the spine and hip of ovariectomized monkeys: a head-to-head comparison with alendronate. *Bone* 56(2):489–496.
- Wilson T, Hastings JW. 1998. Bioluminescence. *Annu Rev Cell Dev Biol* 14:197–230.
- Wise LD, Winkelmann CT, Dogdas B, Bagchi A. 2013. Micro-computed tomography imaging and analysis in developmental biology and toxicology. *Birth Defects Res C Embryo Today* 99(2):71–82.
- Wise LD, Xue D, Winkelmann CT. 2010. Micro-computed tomographic evaluation of fetal skeletal changes induced by all-trans-retinoic acid in rats and rabbits. *Birth Defects Res B Dev Reprod Toxicol* 89(5):408–417.
- Wolf F, Li W, Li F, Li C-Y. 2011. Novel luciferase-based reporter system to monitor activation of ErbB2/Her2/neu pathway noninvasively during radiotherapy. *Int J Radiat Oncol Biol Phys* 79(1):233–238.